PUB-74-113
E-0001

Exp. #1A

Further Observation of Muonless Neutrino-Induced Inelastic Interactions*

B. Aubert†, A. Benvenuti, D. Cline, W. T. Ford, R. Imlay, T. Y. Ling, A. K. Mann, F. Messing, R. L. Piccioni,** J. Pilcher***, D. D. Reeder, C. Rubbia, R. Stefanski and L. Sulak

Department of Physics
Harvard University
Cambridge, Massachusetts 02138

Department of Physics
University of Pennsylvania
Philadelphia, Pennsylvania 19104

Department of Physics
University of Wisconsin
Madison, Wisconsin 53706

National Accelerator Laboratory
Batavia, Illinois 60510

APR 3 1974
FNAL LIBRARY

Abstract

We report here additional positive results of a search for muonless neutrino and antineutrino induced events using an enriched antineutrino beam and a muon identifier of relatively high geometric detection efficiency. The ratio of muonless to muon event rates is observed to be R = 0.20 ± 0.05. We observe no background derived from ordinary neutrino or antineutrino interactions that is capable of explaining the muonless signal.

The investigation reported here is a search for high energy inelastic neutrino and antineutrino interactions that differ from the usual processes by the absence of a muon in the final state. A previous search for such events by us[1] yielded a positive signal. To test the validity of that experiment the original detector was modified significantly and new data were taken which are presented here.

The experiment was carried out at the National Accelerator Laboratory, where collisions of 300 GeV protons with an aluminum target produced secondary hadrons that were focussed by a single magnetic horn to provide a beam enriched in antineutrinos.[2] The experimental apparatus (Fig. 1a) is a modified version of the arrangement described previously.[1,3] The modifications are: 1) the addition of 35 cm of iron immediately downstream of the ionization calorimeter to form a muon identifier (μ_1) consisting of counter B and spark chamber 4 and 2) doubling of the area of counter C and replacement of the 5.3 m^2 narrow-gap spark chambers in the magnetic spectrometer with 8.4 m^2 wide-gap chambers to increase the solid angle of the second (original) muon identifier (μ_2).

The experiment was triggered by the deposition of energy (E) in the ionization calorimeter greater than a preset minimum value,[4] with counter A in anticoincidence. The hadron cascade of an actual event is illustrated in Fig. 1b and the track pattern observed in spark chambers SC1-SC8 is illustrated in Fig. 1c which shows one of the three stereoscopic views of the event. Events were verticized by extrapolation of tracks in the two ±7.5° stereo views and

in the 90° stereo view, and consistency was required between the z-position obtained from the visual reconstruction of the vertex and the calorimeter pulse height information.

The z-dependence of all triggers was observed to be uniform except for a small excess of events in the first segment (module) of the target-detector, which is consistent with the small (5%) geometrical inefficiency of counter A. There is no evidence of neutrons or photons, unaccompanied by charged particles, entering the front of the target. Since each segment of the calorimeter corresponds to approximately 0.6 nuclear collision lengths, to provide additional protection from penetrating hadrons, events occurring upstream of module 5 were excluded. A further restriction, $z \leq 12$, was imposed to reserve 4 modules for detection of the hadronic cascade and as additional absorber for μ_1.

Events can be tentatively classified as having a muon or not according to the response of scintillation counter B, and are labeled $\overline{A}EB$ and $\overline{A}E\overline{B}$, repectively. In Fig. 2 are shown the distributions in hadron energy, E_H, for the 1410 triggers in the z fiducial region. The shaded histograms show those events for which a hadron shower with a reconstructed vertex was present in the spark chambers. Except for very low energy $\overline{A}E\overline{B}$ triggers, about two-thirds of the events have a reconstructed vertex.[5] The remainder can be accounted for in the main by neutrino interactions in the calorimeter beyond the spark chamber boundaries. The larger excess of low-energy $\overline{A}E\overline{B}$ triggers appears to be diffuse showers that originate outside the target of which only traces are seen in

the spark chambers.

The distribution of shower vertices in the transverse plane is nearly uniform, with a small depletion toward the target boundary consistent with the neutrino beam r.m.s. radius of $\sim$1.5 meters. A fiducial boundary limit of ±120 cm in x and y was imposed to avoid regions of low detection efficiency and to insure complete rejection of hadrons entering the sides.[6] A total of 535 events passed the threshold on E_H and satisfied the criteria on vertex location, event quality and time of occurrence within the beam gate.

To use counter B or SC4 as a muon identifier it is necessary to measure the probability ε_p that hadrons penetrate the μ_1 absorber. A sample of events with muons identified by the counter configuration $\bar{A}EBC$ were used to measure the penetration (punch-through) probability of the accompanying hadrons as a function of the z-position of the event vertex (Fig. 3a), and as a function of the energy of the hadronic shower (Fig. 3b). The shapes of these dependences are consistent with other measurements[7] of hadron penetration as indicated in Figs. 3a and 3b.

The angular distribution of muons[8] identified by a spark in SC4 (for about 2/3 of the muon sample) is shown as the histogram in Fig. 3c, after correction for the geometric acceptance of SC4. The geometric acceptance of SC4 is calculated using only the observed distributions of event vertex positions and assuming azimuthal symmetry of the primary neutrino interaction. The raw data divided by the calculated acceptance yield directly the intrinsic

muon angular distribution in Fig. 3c. Calculations which use the measured neutrino-antineutrino spectrum and a model of the interaction dynamics[3] yield the intrinsic muon angular distribution shown by the solid curve in Fig. 3c. We conclude from the good agreement in Fig. 3c that these latter calculations reproduce the observed angular distribution out to the maximum detected angle of 500 mrad. Only 4% of the muons are predicted to lie at angles greater than 500 mrad. The muon detection efficiency, ε_μ, is then obtained from the measured angular distribution, corrected for the loss of events with $\theta_\mu > 500$ mr.[9]

The ratio of muonless events to events with muons is obtained from the formula

$$R = \frac{[\varepsilon_\mu + \varepsilon_p - \varepsilon_\mu \varepsilon_p](1 + R_m) - 1}{1 - \varepsilon_p(1 + R_m)} \qquad (1)$$

where R_m is the measured ratio of events without and with a count in a given muon identifier. In Fig. 3d we plot the observed fraction of events with a muon as a function of z and of (x, y), after correction for hadron punch-through, which should be equal to ε_μ if R = 0 (eq. 1). The data were obtained using SC4 alone as a muon identifier (μ_1'), and are to be compared with ε_μ, shown as the cross-hatched regions in Fig. 3d. A clear discrepancy is indicated, providing evidence that R is different from zero.

Figures 4a, 4b and 4c present R as a function of (a) the transverse position of the event vertex, (b) the z-position of the event vertex, and (c) the hadron energy, E_H. We have included in Fig. 4 results for SC4 alone (μ_1'), as well as for μ_1 and μ_2. The

best solid angle is achieved with μ_1, but for μ_1' the measured values of ε_p are smaller than for μ_1 (Fig. 3b), and for μ_2, ε_p = 0. Furthermore, the dependence on z, (x, y) and E_H of the ε_μ for μ_1, μ_1' and μ_2 is significantly different, which serves to test the internal consistency of the data.[10] Apart from statistical fluctuations, Fig. 4 indicates that the same value of R is obtained from each of the muon identifiers over the entire range of each of the variables plotted and provides evidence for stability of the results. These results integrated over z, transverse position and E_H yield

$$R = 0.20 \pm .05,$$

where the error includes an estimate of 0.03 for uncertainty in the magnitude of ε_μ and ε_p.

The value of R measured for the combined neutrino-antineutrino beam used in this experiment is related to the values of R^ν and $R^{\bar{\nu}}$, for pure neutrinos and antineutrinos, respectively, by

$$R = aR^\nu + (1 - a)R^{\bar{\nu}},$$

where a = 0.63 ± 0.11 is the corrected observed ratio of the negative muon event rate to the total muon event rate. The allowed values of R^ν and $R^{\bar{\nu}}$ are presented in Fig. 4d which also shows the recent results for R^ν and $R^{\bar{\nu}}$ from CERN.[11]

In summary, this experiment, which includes a number of tests of its internal consistency and uses mainly directly measured quantities in making necessary corrections to the data, yields an excess of muonless events, in agreement with our earlier experiment.[1]

It is a pleasure to acknowledge the aid and encouragement of

the National Accelerator Laboratory staff amd the efforts of Robert Beck and Hans Weeden.

Footnotes and References

*Supported in part by the U. S. Atomic Energy Commission under Contract AT(11-1)-881-401.

†On leave of absence from Laboratoire de L'Accelerateur Lineaire, Orsay, France.

**Now at Stanford Linear Accelerator Center, Stanford, California 94305.

***Alfred P. Sloan Foundation Fellow, now at the University of Chicago, Chicago, Illinois 60637.

1. A. Benvenuti et al., to be published in Phys. Rev. Letters.
2. The horn was constructed under the supervision of F. Nezrick.
3. A. Benvenuti et al., Phys. Rev. Letters 30, 1084 (1973), 32 125 (1974).
4. The triggering circuitry was determined from the data to be fully efficient for hadron energy $E_H > 4$ GeV. In the analysis we have imposed a cut at this energy to guarantee a sharp threshold.
5. For $\overline{A}E\overline{B}$ triggers the ratio of verticized events to all events is 0.22 for $E_H < 12$ GeV and 0.57 for $E_H > 12$ GeV, for $\overline{A}EB$ events the corresponding ratios are 0.57 and 0.74.
6. As Fig. 3d shows, the data do not indicate any excess of muonless events near the edges (142 cm) of the detector.
7. R. W. Ellsworth et al., Phys. Rev. 165, 1449 (1968).

8. The angle of the muon is determined from the angle of the 10 cm long track segment in SC4 and from the line joining the track centroid to the shower vertex. By requiring consistency of these measurements we eliminate nearly all penetrating hadrons.

9. The detection efficiency, ε_μ, includes a small correction ($\sim$0.3%) for muons within the angular acceptance that range out.

10. For muon identifiers μ_1, μ_1', and μ_2 the average ε_μ are 0.89, 0.81 and 0.79; the corresponding average ε_p are 0.21, 0.14 and 0. The small geometric inefficiency of counters B and C is reduced to less than 1% by using track information from SC4 and SC5.

11. F. J. Hasert et al., Phys. Letters 46B, 138 (1973), and CERN preprint TC-L/Int. 74-1, to be published.

Figure Captions

Fig. 1 (a) Plan view of the modified experimental apparatus. The target detector consists of liquid scintillator segments (1-16) with wide-gap spark chambers (SC1-SC4) interspersed. The muon spectrometer includes SC5-SC8. Auxiliary scintillation counters are A, B, C and D. An inelastic neutrino event with an associated muon is sketched into the spark chambers (c) and the energy deposition in each segment is shown in (b).

Fig. 2 (a) The E_H distribution of all $\overline{A}EB$ triggers and of the corresponding verticized events (cross-hatched).

(b) The E_H distribution of all $\bar{A}E\bar{B}$ triggers and the corresponding verticized events (cross-hatched).

Fig. 3 (a) The measured punch-through probability of hadrons accompanying $\bar{A}EBC$ events (for all hadron energies) as a function of z, and the expected shape of the distribution.

(b) The measured punch-through probability (for z between 5 and 12) as a function of E_H, compared with the expected variation.

(c) The corrected muon angular distribution measured in SC4 compared with the predicted distribution.

(d) Comparison of the observed fraction of events with a muon for the μ_1' identifier (SC4 alone) and ε_μ as functions of transverse position and z-position. The cross-hatching indicates the uncertainty in ε_μ arising from the statistics of the data in Fig. 3c.

Fig. 4 (a) R obtained from three different muon identifiers as a function of the transverse distance from the center of the calorimeter.

(b) The z-variation of R obtained using three different muon identifiers. Each calorimeter unit corresponds to 0.6 nuclear collision lengths.

(c) The E_H variation of R from three muon identifiers.

(d) The allowed region of R^ν and $R^{\bar{\nu}}$ from this experiment compared with R^ν and $R^{\bar{\nu}}$ obtained in the CERN measurement.

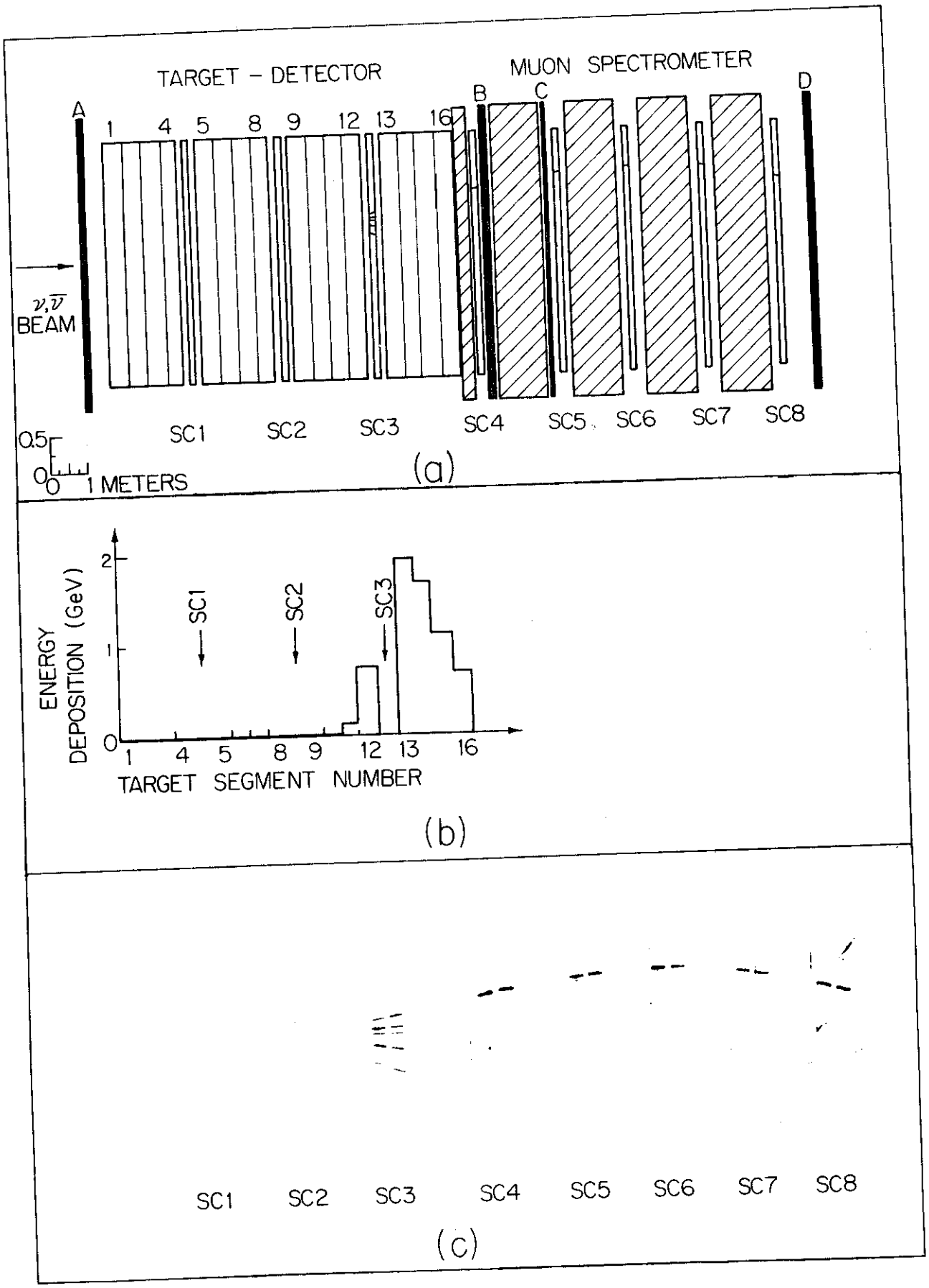
TARGET - DETECTOR
MUON SPECTROMETER
A
B
C
D
1 4 5 8 9 12 13 16
ν,ν̄
BEAM
SC1 SC2 SC3 SC4 SC5 SC6 SC7 SC8
0.5
0 1 METERS
(a)
ENERGY DEPOSITION (GeV)
2
1
0
SC1
SC2
SC3
1 4 5 8 9 12 13 16
TARGET SEGMENT NUMBER
(b)
SC1 SC2 SC3 SC4 SC5 SC6 SC7 SC8
(c)

Fig. 1a, 1b & 1c

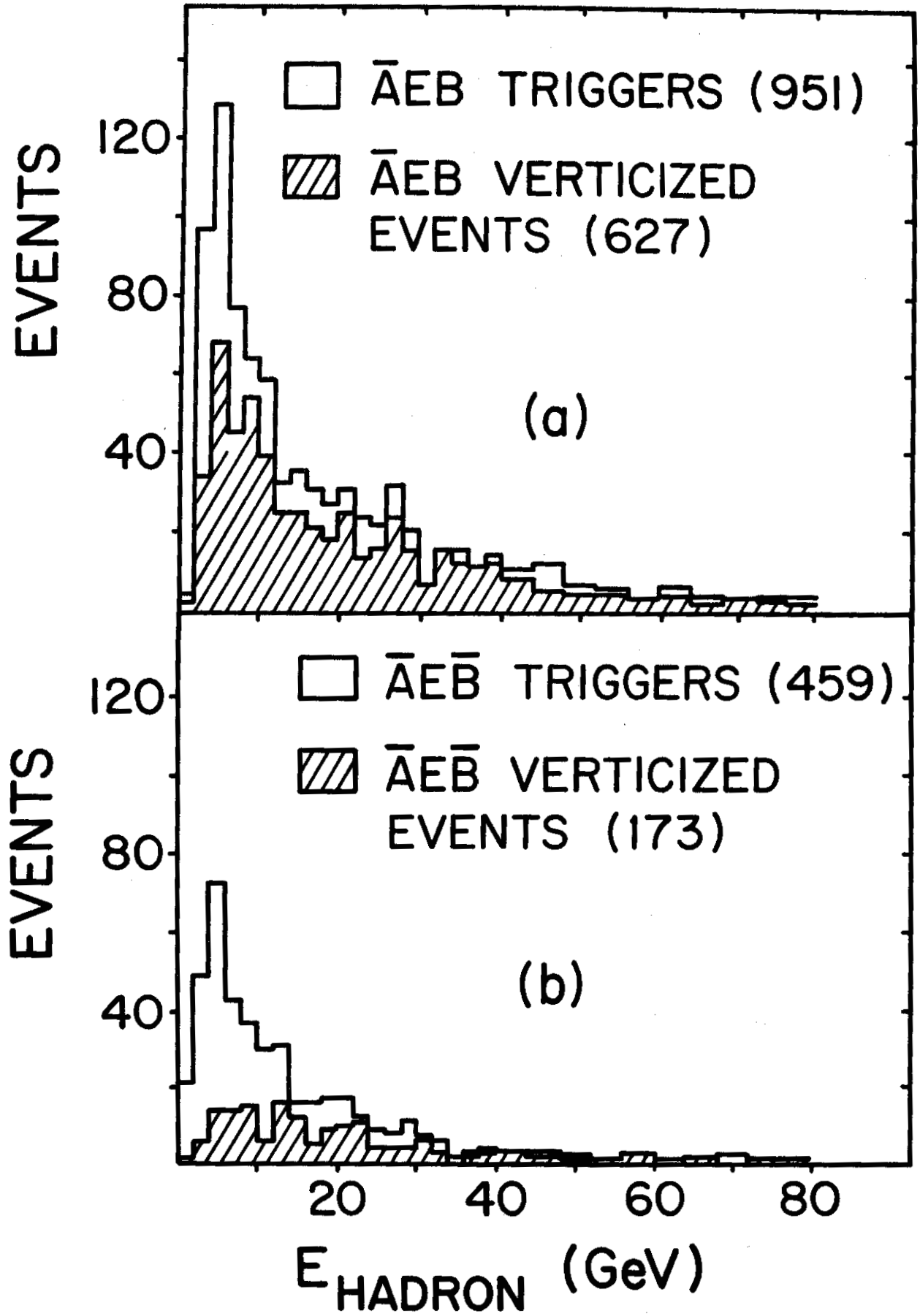
ĀEB TRIGGERS (951)
ĀEB VERTICIZED EVENTS (627)
(a)
ĀEB̄ TRIGGERS (459)
ĀEB̄ VERTICIZED EVENTS (173)
(b)
EVENTS
120
80
40
20
40
60
80
E HADRON (GeV)

Figs. 2a & 2b

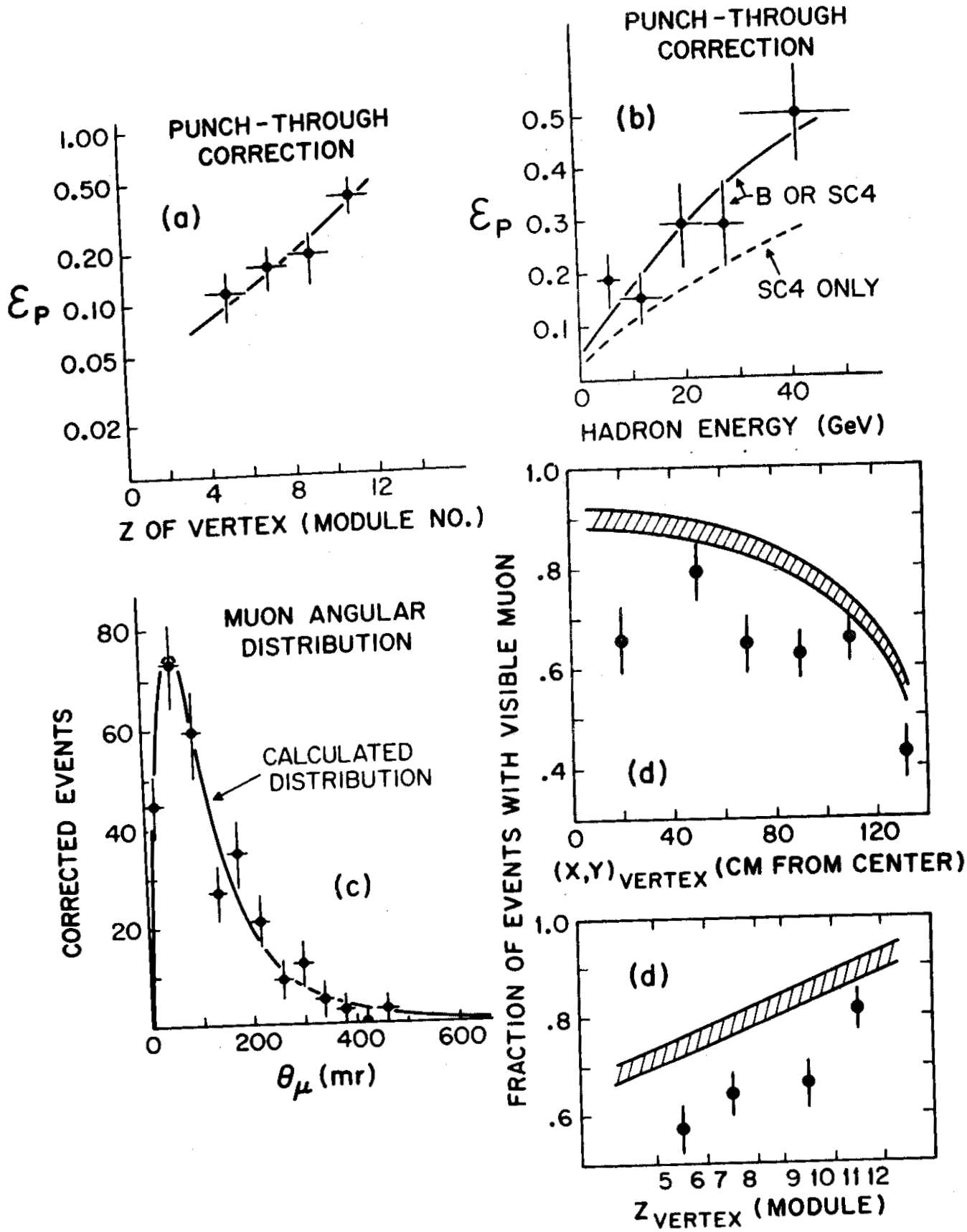

Figs. 3a, 3b, 3c & 3d

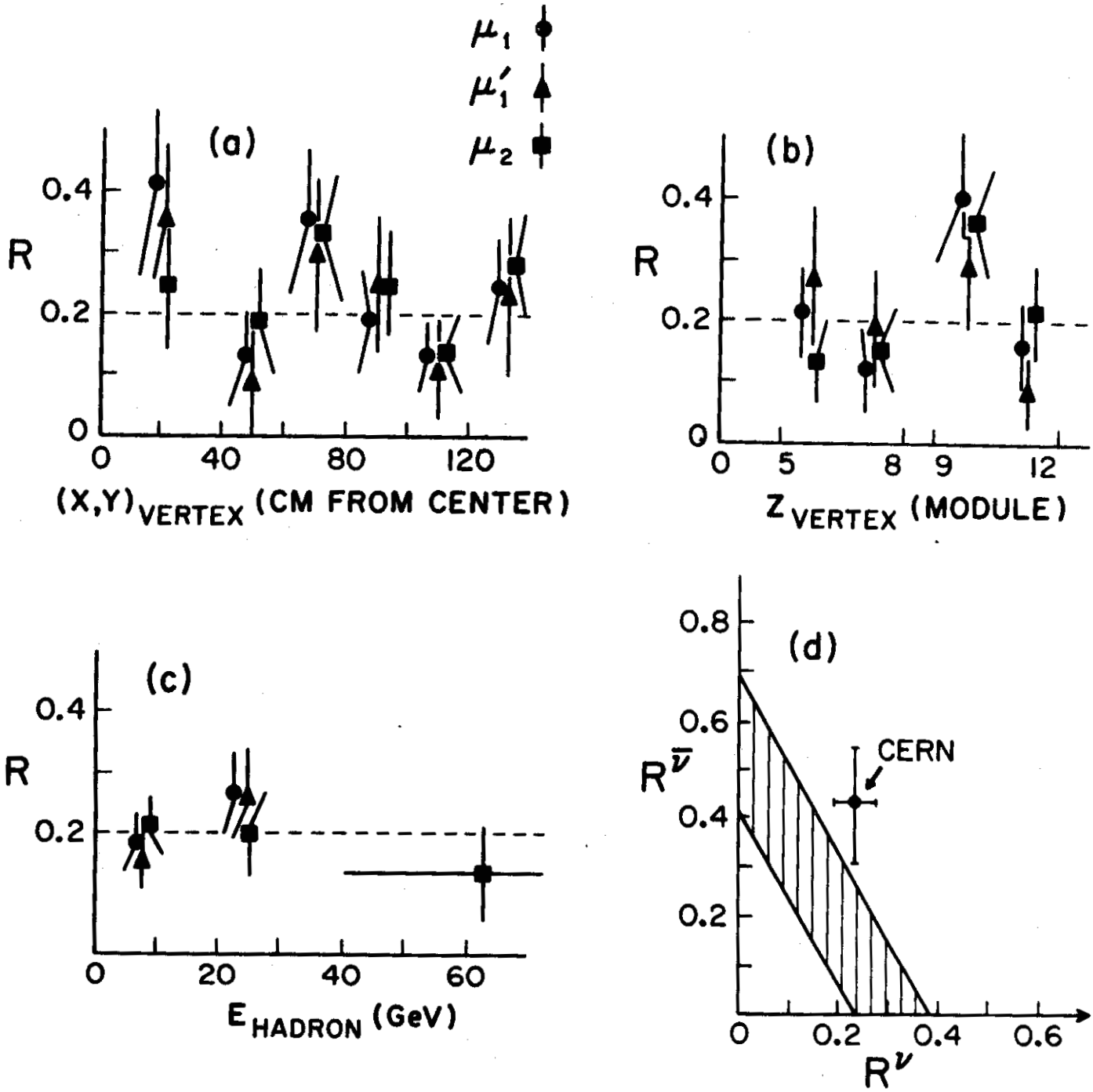

Figs. 4a, 4b, 4c & 4d